Photosynth Res (2017) 131:79–91
DOI 10.1007/s11120-016-0300-8

ORIGINAL ARTICLE

In vitro kinetics of P_{700}^+ reduction of *Thermosynechococcus elongatus* trimeric Photosystem I complexes by recombinant cytochrome c_6 using a Joliot-type LED spectrophotometer

Khoa Nguyen[1] · Michael Vaughn[1,2] · Paul Frymier[3,4,5] · Barry D. Bruce[1,3,4,5]

Received: 10 June 2016 / Accepted: 11 August 2016 / Published online: 13 October 2016
© Springer Science+Business Media Dordrecht 2016

Abstract The reduction rate of photo-oxidized Photosystem I (PSI) with various natural and artificial electron donors have been well studied by transient absorption spectroscopy. The electron transfer rate from various donors to P_{700}^+ has been measured for a wide range of photosynthetic organisms encompassing cyanobacteria, algae, and plants. PSI can be a limiting component due to tedious extraction and purification methods required for this membrane protein. In this report, we have determined the in vivo, intracellular cytochrome c_6 (cyt c_6)/PSI ratio in *Thermosynechococcus elongatus* (*T.e.*) using quantitative Western blot analysis. This information permitted the determination of P_{700}^+ reduction kinetics via recombinant cyt c_6 in a physiologically relevant ratio (cyt c_6: PSI) with a Joliot-type, LED-driven, pump-probe spectrophotometer. Dilute PSI samples were tested under varying cyt c_6 concentration, temperature, pH, and ionic strength, each of which shows similar trends to the reported literature utilizing much higher PSI concentrations with laser-based spectrophotometer. Our results do however indicate kinetic differences between actinic light sources (laser vs. LED), and we have attempted to resolve these effects by varying our LED light intensity and duration. The standardized configuration of this spectrophotometer will also allow a more uniform kinetic analysis of samples in different laboratories. We can conclude that our findings from the LED-based system display an added total protein concentration effect due to multiple turnover events of P_{700}^+ reduction by cyt c_6 during the longer illumination regime.

Keywords Photosystem I · Cytochrome c_6 · Electron transfer · Flash photolysis · JTS-10 · P700 · *Thermophilic cyanobacteria*

In memory of our Friend, Colleague, and Mentor, Dr. David B. Knaff.

Electronic supplementary material The online version of this article (doi:10.1007/s11120-016-0300-8) contains supplementary material, which is available to authorized users.

✉ Barry D. Bruce
bbruce@utk.edu

[1] Department of Biochemistry & Cellular and Molecular Biology, University of Tennessee, Knoxville, TN 37996, USA

[2] Department of Chemistry, Arizona State University, Tempe, AZ 85287, USA

[3] Department of Biomolecular and Chemical Engineering, University of Tennessee, Knoxville, TN 37996, USA

[4] Sustainable Energy and Education Research Center, University of Tennessee, Knoxville, TN 37996, USA

[5] Bredesen Center for Interdisciplinary Education and Research, University of Tennessee, Knoxville, TN 37996, USA

Introduction

In oxygenic and anoxygenic photosynthetic organisms, photosynthetic electron transport requires a soluble electron carrier protein to couple the process of electrogenic proton pumping via the b_6f/bc_1 membrane complex with the light-activated charge separation associated with the reaction center of Photosystem I (Blankenship 2002). In oxygenic cyanobacteria and algae, two separate metalloproteins have evolved to perform this physiological role, a heme-containing protein, cytochrome c_{553} (also called cyt c_6), and a type 1 copper protein, plastocyanin (PC) (Wood 1978). Despite no sequence or structural similarities, both proteins have reversible 1-electron metal redox centers and are capable of binding to the luminal side of PSI in the

thylakoid membrane and donating an electron to P_{700}^{+} (Bohner et al. 1980). Although functionally interchangeable, cyt c_6 is considered to be the original, ancestral protein and is still found in primitive, thermophilic cyanobacteria (Beissinger et al. 1998, Nakamura et al. 2002). However, as iron became limited in aquatic environments following the great oxygenic event (Hervas and Navarro 2011), evolution yielded an alternative, copper-containing electron donor, PC, which reduced the dependence of these photosynthetic organisms on scarcely available iron. In some algae both cyt c_6 and PC genes still exist with PC being primarily expressed under iron-limiting conditions (Ho and Krogmann 1984). In vascular plants only PC has been shown to reduce PSI, although there is a cyt c_6-like protein expressed in *Arabidopsis* (Gupta et al. 2002), and this protein is unable to donate electrons to P_{700}^{+} (Molina-Heredia et al. 2003) .

Direct reduction of the oxidized special pair (P_{700}^{+}) by these soluble donors occurs on the luminal surface of PSI. This electron transfer step has been previously studied with a variety of eukaryotic and prokaryotic systems, both in vivo and in vitro with isolated proteins, along with artificial donors to P_{700}^{+} (Gourovskaya et al. 1997; De la Rosa et al. 2002; Baker et al. 2014). Previous kinetic models have suggested that there are three mechanisms for P_{700}^{+} reduction by either PC or cyt c_6: oriented collision, complex formation, and complex formation with interface rearrangement (Hervas et al. 1995). These models have been proposed as evolutionary intermediates in the optimization of surface interactions between donor and acceptor proteins, with less specificity in cyanobacteria systems increasing affinity in the interactions of algal and higher plant systems (Hippler et al. 1999; Olesen et al. 1999; Hervas et al. 2003, 2005).

The rate of P_{700}^{+} reduction has been characterized mainly by laser-based flash absorption spectroscopy at various wavelengths, characteristic of either donor or acceptor proteins (Hervas et al. 1992; Mamedov et al. 1996; Olesen et al. 1999). Reported rate constants vary from micro- to millisecond lifetimes with varying interpretations fitting with single, biphasic (Diaz-Quintana et al. 2003), and three component (Jin et al. 2001) exponential models typically under pseudo-first-order kinetics. Moreover, this variation still holds even when comparing the kinetics of different cyanobacterial systems, where multiphasic rate differences are dependent on species, measurement apparatus, protein concentration, temperature, ionic strength, and mutations of protein surface charges (Hatanaka et al. 1993; Hippler et al. 1998; Balme et al. 2001).

In this work we have characterized the in vitro kinetics of P_{700}^{+} reduction using purified PSI and recombinantly expressed cyt c_6 from the thermophilic cyanobacteria *Thermosynechococcus elongatus*. In order to determine the relevant range of the intracellular cyt c_6 to PSI ratio, we have also conducted a quantitative Western blot analysis using known amounts of purified recombinant cyt c_6 and PSI subunits (PsaD and PsaF) that were used to standardize the signal from intact *T. elongatus* cells probed with polyclonal antibodies (α-PsaD, α-PsaF, α-cyt. c_6) (S. Fig. 1 and Fig. 1).

The in vitro flash photolysis characterization was then performed using a Biologic JTS-10, a Joliot-type LED pump-probe spectrophotometer (Biologic SAS, Claix, France). Similar to traditional laser-based flash photolysis systems, the JTS utilizes an actinic source of light to photo-oxidize (bleach) the special pair chlorophyll, P700, of PSI. The sample cuvette is positioned in front of the main detector that has a 705 nm filter, which only experiences the probe light (705 nm) and not the actinic beam. The probe beam is also split so that a secondary reference detector sees the same amount of detection light as the main detector, minus what is absorbed by the sample. The probing of the detection light allows us to monitor the amount of light being absorbed by P700 before and after the actinic flash. The recovery of the $Abs_{705\ nm}$ curve back to the pre-actinic flash baseline indicates that the photo-oxidized P700 is being reduced by cytochrome c_6 ($P700^{+} \rightarrow P700$) .

Although this instrument does not have the kinetic resolution of laser-based systems with shorter actinic flashes, it is capable of resolving the cytochrome c_6 reduction kinetics of *T. elongatus* P_{700}^{+} as a recovery from the bleaching of the ground state at 705 nm or as the appearance of the absorbance of P_{700}^{+} at 810 nm. The compact size, ease,

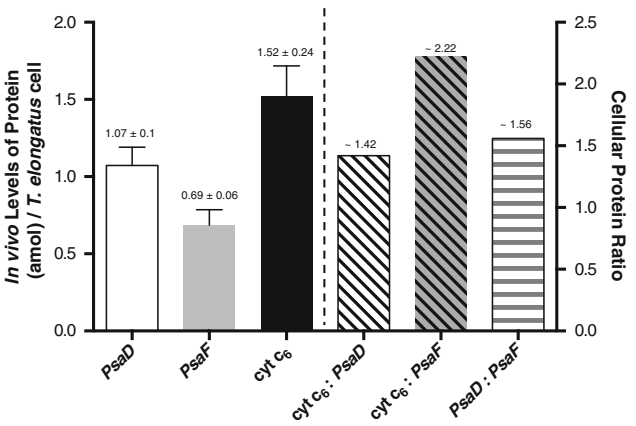

Fig. 1 Quantification of Western blot analysis for cellular content of PSI (PsaD/PsaF) and cytochrome c_6 in *T. elongatus*. On the left *y*-axis, PsaD (*solid white bar*) was estimated to populate a *T. elongatus* cell at a concentration of 1.07 ± 0.1 amol, PsaF (*solid gray bar*) at 0.69 ± 0.06 amol, and cyt c_6 (*solid black bar*) at 1.52 ± 0.24 amol. The resulting cellular ratio (right *y*-axis) of cyt c_6 to PsaD (*white with black stripes bar*) is estimated to be 1.4, cyt c_6 to PsaF (*gray with black stripes bar*) at 2.2, and PsaD to PsaF (*white with gray stripes bar*) at 1.56

affordability, and high sensitivity of this instrument make it ideal for measuring many of the parameters that affect the kinetics of electron transport in vitro and possibly in the field. The common design and solid-state nature of the JTS-10 will permit many labs to compare results using a common instrument. We have been able to determine the effect of donor concentration, temperature, ionic strength, pH, and total protein on this electron transfer process. The reduction kinetics fit well to a two-phase recovery with half-lives of the fast and slow phase of 6.7 and 62.3 ms, respectively (Fig. 5a, 10:1 trace). We are currently exploring models to explain the observed two-phase kinetics. In addition, through site-directed mutagenesis we are making selective amino acid changes that may increase the affinity and stability of interactions between the PsaF (lumenal PSI subunit) and cyt c_6. Since we are working in vitro we do not need to be constrained by the physiological need to cycle between the b_6/*f* complex and PSI, thus we can maximize the interaction between PSI and cyt c_6 and thereby enable higher yield of either photosynthetic hydrogen production or photocurrents in vitro.

Materials and methods

Growth of *T. elongatus*

The thermophilic cyanobacterium *T. elongatus BP*-1 was grown in 2-l airlift fermenters (Bethesda Research Labs) in BG-11 media. The temperature was held between 50 and 55 °C with continuous illumination by fluorescent lights. The light level was adjusted as the cultures approached higher densities to a maximum of 50 E μm^{-2} s^{-1}. Cells were pelleted during late log phase by centrifugation for 15 min at 7500×*g*.

PSI isolation and recombinant cytochrome c_6 expression/purification

PSI particles from *T. elongatus* were isolated and purified using sucrose density gradient centrifugation (S. Fig. 5) and anion exchange chromatography as described in Iwuchukwu et al. (2010). Recombinant *T. elongatus* cytochrome c_6 was co-expressed with the maturation pathway for c-type cytochromes in *E. coli* and purified from the periplasm as described in the previous work (Kranz et al. 1998).

PSI antibody production

The psaD and cyt c_6 gene was cloned from *T. elongatus* genomic DNA. A synthetic codon-optimized DNA fragment encoding the psaF gene from *T. elongatus* was purchased (Epoch Life Science, Inc., Missouri City, TX). Both psaD and psaF sequences were cloned into pTYB2 vector, and the gene product was expressed and purified from *E. coli* using the IMPACT system (New England Biolabs, Ipswich, MA). Polyclonal antibodies were produced in rabbits (Pocono Rabbit Farm, Canadensis, PA) following immunization and boosting with the recombinant cytochrome c_6, PsaD, and PsaF.

Western blots

Western blot analysis was performed on *T. elongatus* intact whole cells along with recombinant proteins separated using the same 15 % SDS-PAGE gel and transferred onto Immobilon-P Transfer Membrane (Millipore) using a graphite electroblotter (Idea Scientific, Minneapolis, MN). Immobilon-P was blocked for 3 h in TBS buffer with 0.1 % Tween-20, 2 % BSA, and 2 % NFM. After blocking, incubation with primary antibodies (α-PsaD 1:50,000, α-PsaF 1:10,000, α-cyt. c_6 1:5000) was done in the same buffer overnight at 4 °C. Three washes with TBS-Tween (2 % NFM) were performed before a 1 h incubation with a goat anti-rabbit IgG HRP secondary antibody (1:50,000). Final visualization was achieved with SuperSignal West Dura Extended Duration Substrate (Thermo Scientific).

For each antigen a standard curve of four concentrations was used and a range of cell numbers was tested on a single blot. This permitted a standard curve to be generated and 3–4 independent concentrations determined. All measurements were repeated three times to provide a final *N*-value of 12–15 for each antigen.

JTS-10 configuration and data collection

Basic configurations of JTS utilize an "Orange Ring" array of LEDs (630 nm peak emission) for the actinic source at 3000 μE m^{-2} s^{-1} intensity (unless otherwise noted), with the probe LEDs either at 705 or 810 nm (including interference filters at the respective wavelengths). Data collection consists of 15 discrete points (500 ms apart) to establish a pre-actinic flash baseline, followed by 200 points of post-actinic flash, exponentially increasing from 60 μs to 10 s. The first 15 points (pre-actinic flash) and the last 10 points are used for a linear regression of each sample trace (S. Fig. 2). Data shown are an average of three individual traces with a subtraction of a non-actinic trace, accounting for any actinic activity given off by the probe LEDs. Data analysis and curve fitting were performed using GraphPad Prism ®software.

Sample set-up for JTS-10

Samples comprised purified *T. elongatus* PSI at 3 μg chlorophyll/ml or ~35 nM (assuming 96 chl a/PSI), with a

ten-fold molar excess of recombinantly expressed *T. elongatus* cytochrome c_6 as described previously (Iwuchukwu et al. 2010). The sample mix also includes 2 mM sodium ascorbate, 0.1 mM methyl viologen, 5 mM $MgCl_2$, 5 mM $MgSO_4$, brought up to 1 mL of 20 mM MES buffer (pH 6.4) with 0.03 % *n*-dodecyl-β-D-maltoside (Glycon Biochemicals, Germany).

Laser flash photolysis

Kinetic experiments at 830 nm were performed on an in-house constructed system similar to that of (Xu et al. 2003). For the detection beam, a Newport 150 mW diode was used. For single-turnover excitation, a Spectra Physics Q-switched Nd:YAG laser was frequency doubled to 532 nm to provide a saturating laser flash with pulse width of 6–9 ns. The power of each laser pulse reaching the sample and the light reaching the detector was limited using neutral density filters. Datasets were averaged 8–32 times with 5 s between each laser flash. Signals were detected with an OSI Optoelectronics PIN-10D photodiode and were amplified using a Femto DHPCA-100 High Speed Variable Gain Amplifier. Signals were digitized and recorded using a Tektronix 3012B oscilloscope and a LabView® program written in-house. Datasets were fitted with 1st, 2nd, and 3rd order exponential models in Prism®.

Results

Western blot quantification of intracellular Cyt c_6 and PSI ratio

In order to quantify and compare the intracellular concentration of PSI and cytochrome c_6, we cannot directly look at the Western blots of the intact cells alone since many variables like primary antibody specificity, slight variations in SDS gel running, and blot exposure time will affect the signal intensities of the bands. Instead, known amounts of the respective recombinant proteins are ran on the same gel as the intact cells, allowing a direct comparison to standards going through the exact blotting conditions.

To generate these standard curves, recombinant cyt c_6 (20–160 ng) was ran on the same SDS-PAGE as *T. elongatus* cells (1–8 × 10^6), which was then blotted using α-cyt c_6 (S. Fig. 1a–b) and quantified using NIH ImageJ (S. Fig. 1c–d). From here, four independent concentrations of cyt c_6 per *T. elongatus* cell were calculated giving an average value of 1.52 ± 0.24 amol/cell of cyt c_6 (1e). The same technique was repeated for PsaD (α-PsaD) (S. Fig. 1 f–j) and PsaF (α-PsaF) (S. Fig. 1k–o), yielding 1.07 ± 0.1 *and* 0.69 ± 0.06 amol/cell, respectively (S. Fig. 1j and o). The resulting values are shown in Fig. 1 (left *y*-axis), along with the cellular protein ratio (right *y*-axis). The cyt c_6 to PsaD and to PsaF ratios (Fig. 1) were calculated to 1.42 (white bar with black stripes), 2.22 (gray bar with black stripes), respectively. The PsaD to PsaF was calculated to be 1.56 for PSI. We suspect that PsaD, being on the stromal hump of PSI, has the potential to be in greater quantity than the thylakoid-bound PsaF, which would have a less frequent turnover time while in the membrane.

The only intracellular concentration of PSI that we found was calculated for *Synechocystis* 6803 via chlorophyll extrapolation, which resulted in about 96000 units per cell (Keren et al. 2004). Considering the values we calculated for psaD (15.24 kDa) and psaF (17.7 kDa) (1.07 and 0.69 amol, respectively), along with an estimated cell volume of 1.5 × 10^{-14} L, the resulting average of PSI units per cell was about 530,000. Using the same cellular volume and 1.52 amol, cyt c_6 (11.8 kDa) came to about 915,000 units per cell. With *Synechocystis* 6803 being a mesophile and our *T. elongatus* a thermophile, many factors, including growth conditions, chlorophyll approximation, and cell volume estimation could have contributed to the ×5 difference in intracellular PSI content. This discrepancy however should not affect our resulting relative ratio of the two proteins.

By directly measuring the relative amounts of both PSI (PsaD and PsaF) and the cytochrome c_6 in intact cells using this method, we are able to conclude that the relative ratio of cyt c_6 to PSI is close to the same relative concentrations. Although there are many caveats to making an absolute measurement considering such factors as membrane-excluded space, sub-cellular localization, cellular organization, and possibly macromolecular crowding, to our knowledge, this is the first such reported ratio in a cyanobacteria and is most probably the lowest limit of the ratio due to the caveats described above. Thus we conclude that the ratios of cyt c_6 to PSI used in our experiments were close to the in vivo ratio of about 1.7:1 of cyt c_6 to PSI per *T. elongatus* cell.

LED-based P_{700} photo-bleaching depends on various parameters

Both PSI and cyt c_6 were purified using the methods described previously (Iwuchukwu et al. 2010). The purity of both proteins was determined by SDS-PAGE (Fig. 2a) and BN-PAGE (Fig. 2b). The BN-PAGE indicates that yield and homogeneity of PSI was primarily in the trimeric form at ~ 1068 kDa with very little PSI monomer (~400 kDa) and a very small amount of PSII monomers or dimers (Li et al. 2014). The lack of PSII was also confirmed from the low-temperature fluorescence at 77 K, which had a single prominent peak at 728 nm (Fig. 2c) and

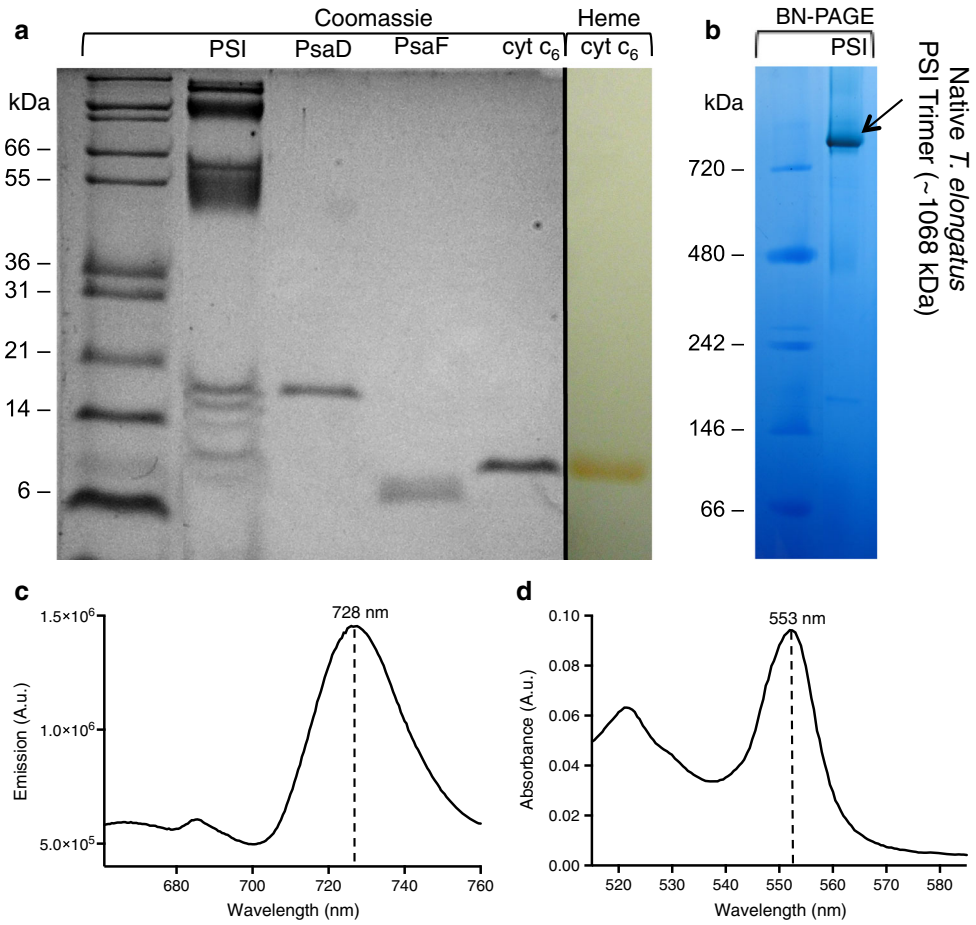

Fig. 2 **a** SDS-PAGE of purified PSI, recombinantly expressed *T. elongatus* PsaD, PsaF (N-term), and cyt c_6 (*left*: coomassie stained and *right*: heme stain). **b** *Blue* Native PAGE of purified *T. elongatus* PSI, showing a high molecular weight band above the 720 kDa band, with *T. elongatus* PSI trimer estimated to be about 1068 kDa (Li et al. 2014). **c** Low-temperature fluorescence scan of PSI, showing a characteristic emission peak at 728 nm. **d** Reduced spectra of cytochrome c_6, with a characteristic peak at 553 nm

lacked the characteristic fluorescent peak at 695 nm (Schlodder et al. 2011). The reduced spectra of cyt c_6 (also c_{553}) showed a characteristic peak at 553 nm as expected (Fig. 2d).

The ability of the JTS-10 to completely photo-oxidize P700 using its LED-based actinic light source was investigated. The amplitude of absorbance change at 705 nm was monitored by varying the length of the LED illumination from 10 µs to 7.5 ms. Fully photo-oxidized samples containing 35 nM PSI (3 µg chlorophyll/ml) displayed a plateau in the intensity of the photo-bleaching after 2.5 ms (Fig. 3a). The actinic LED intensity was also varied from 12 to 3000 µE m^{-2} s^{-1} with three different exposure times (5, 15, and 45 ms). The sigmoidal shape of this light intensity effect on photo-bleaching reached the same saturating value yet took considerable higher light levels when the illumination intensity was reduced from 45 ms to 15 and 5 ms. The complete conversion of P_{700} to P_{700}^+ required a flash duration longer than 5 ms at intensities below 3000 µE/m^2/s as indicated by maximum ΔAbs_{705nm} (Fig. 3b). Considering the required actinic flash duration to reach complete P_{700}^+ formation for this LED-based system is 2–3 ms and previously reported rates of charge separation (approximately 1 µs) to form the (P_{700}^+, F_B^-) pair (Brettel and Leibl 2001), suggests that multiple turnover events of P_{700}^+ reduction by cyt c_6 may be occurring when actinic flash durations in the millisecond range is used. We also tested the effect of the cyt c_6:PSI ratio on the signal intensity. Measurements were performed in triplicate at four concentrations of cyt c_6, ranging between 10- and 60-fold molar excess to PSI, each of which gave similar absorbance amplitudes at each flash duration (Fig. 3a). This indicates that maximum photo-bleaching of our PSI samples were achieved at 5 ms of flash duration, regardless of excess cyt c_6 content. We wanted to ensure that at 5 ms of actinic light exposure, the observed P_{700} oxidation was not limited by the lack of available cytochrome for P_{700} re-reduction.

The sensitivity of the photodiodes used by the JTS-10 allowed P_{700} activity to be measured with very dilute samples. We tested the signal-to-noise of the ΔAbs_{705nm} measurement as a function of P_{700} concentration (Fig. 4a). Using an initial PSI concentration of 544 nM, we diluted the sample two-fold in eight steps to a final concentration of 2.125 nM, taking measurements at each dilution. The reduction curves were then multiplied by the dilution factor

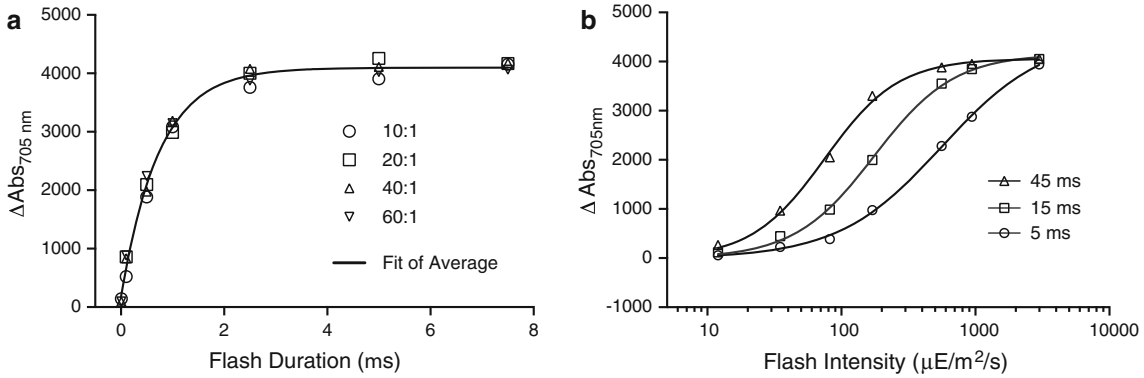

Fig. 3 Total P_{700} photo-oxidation displayed as a function of **a** flash duration and **b** flash intensity. **a** 35 nM of PSI was used with 10-, 20-, 40-, and 60-fold molar excess of cytochrome. **b** 35 nM of PSI was used with a ten-fold molar excess of cytochrome and flash intensity ranged from 12 to 3000 μE/m^2/s

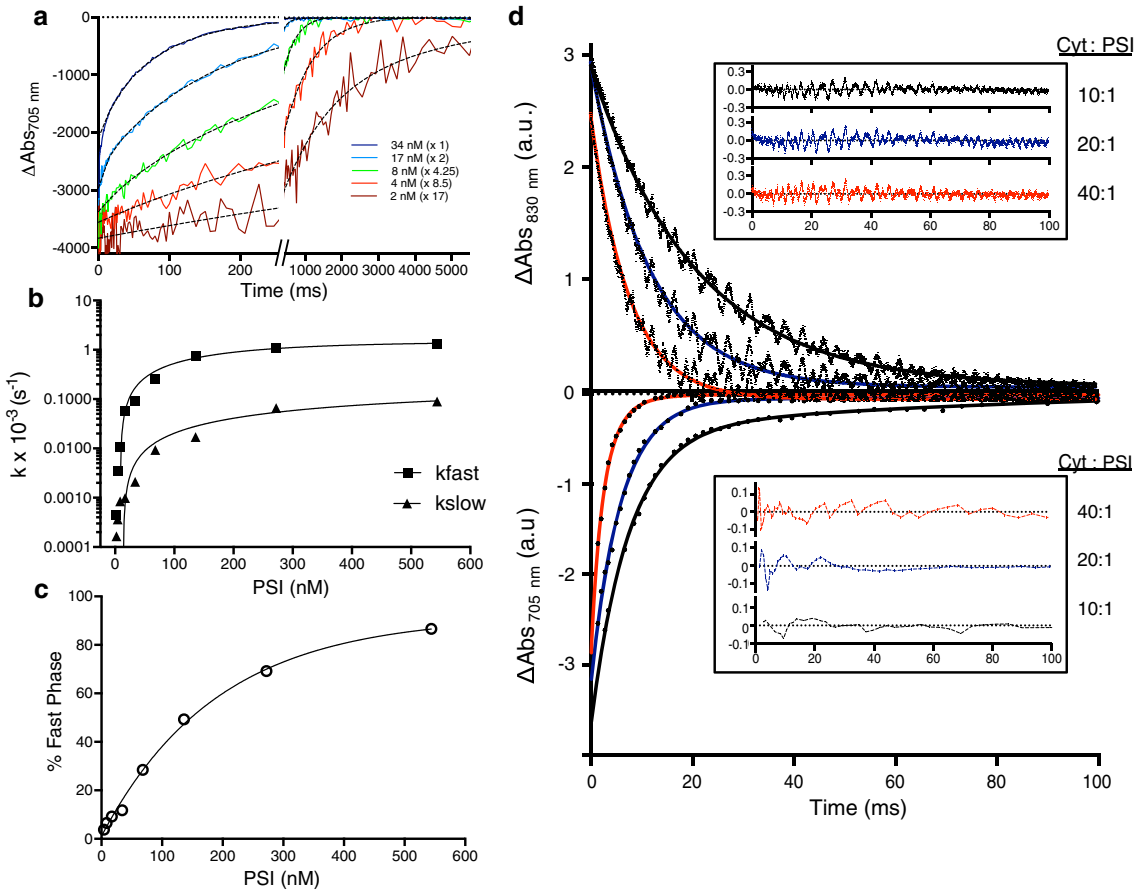

Fig. 4 **a** Raw P_{700} reduction curves, normalized to the dilution factor (cyt:PSI, 10:1) of 34 nM PSI. **b** Rates from two-phase kinetic fits of two-fold dilutions from 544 nM PSI (cyt:PSI, 10:1). **c** Percentage of the fast phase from two-phase kinetic fits of two-fold dilutions from 544 nM PSI (cyt:PSI, 10:1). **d** Recovery curve comparison between actinic sources (top Laser @830 nm vs. bottom-LED @705 nm) at 544 nM PSI with three cyt:PSI ratios shown (10:1, 20:1, and 40:1). The *y*-axis shows both curves normalized to 100 % of the maximal absorbance change. JTS illuminations were kept at a maximal 3000 μE/m^2/s with a duration of 5 ms. The top laser traces were fitted to a 1-phase exponential, while the bottom JTS traces fitted to a 2-exponential. Residuals of each fit are shown in the in-set boxes

to get normalized curves, which were then fitted to a model that is the sum of two exponentials, 34 to 2 nM are shown in Fig. 4a (y-axis normalized to 34 nM amplitude). The two-phase rate constants were reported for each normalized dilution (Fig. 4b), along with the percentage of the fast phase (Fig. 4c). At a 10:1 molar ratio of cyt c_6 to PSI, we

see kinetics sequentially slow down with each dilution along with the percent of the fast phase. We observed P_{700} photo-bleaching and with high-quality data fits of the reduction kinetics all the way down to 0.3 µg chlorophyll ml^{-1}, as the R^2 for 4 nM PSI was still at 0.9848 (Table 1). This is significantly lower concentration of PSI than was used in similar reports in literature range from 10 µg chlorophyll/ml (Hatanaka et al. 1993) (10 × more sensitive) to 0.75 mg chlorophyll ml^{-1} (Hervas et al. 1995) (750 × more sensitive), which indicates the sensitivity of the optical design and photodiodes used in the JTS-10.

Fast phase dependence on methyl viologen concentration was analyzed to ensure that we had provided an adequate amount of electron acceptors (MV) to PSI, allowing for continuous electron flow through the ($P_{700} \rightarrow A_0 \rightarrow A_1 \rightarrow F_X \rightarrow F_A \rightarrow F_B$). Without enough MV to take electrons from the FB iron-sulfur cluster, electrons may travel backwards from F_B to P_{700} (charge recombination). These charge recombination events occur on the tens of milliseconds, depending on where we visualize this re-reduction of P_{700}, where it is reported in literature in various cyanobacteria to be about 20 ms from F_A or 65 ms from F_B (Shinkarev et al. 2002; Santabarbara et al. 2005). We performed a detailed MV titration to confirm this (S. Fig. 3). With PSI kept constant at 35 nm and cytochrome was in ten-fold excess, we see that without methyl viologen there is a distinct fast phase occurring in the tens of milliseconds (S. Fig. 3a). The absolute change in the absorbance of P_{700}, also was greatly affected, with a plateau around 0.1 mM MV (S. Fig. 3b). The percentage of the fast phase without any MV is approximately 43 %, with a steep decrease to about 10 % when even 0.025 mM MV was added, reaching a plateau with additional MV (S. Fig. 3c).

We conclude that the recombination reactions that occur with no final electron acceptor (MV) can be completely alleviated by the addition of as little 0.1 mM MV, as shown by a plateau of P_{700} absorbance and percent fast phase at MV that nears 0.1 mM (S. Fig. 3b–c). Therefore all of our work that was done using 0.1 mM was free from this back reaction.

Table 1 Values from two-phase kinetic fits as shown in Fig. 7b, including the goodness of each fit (R^2)

PSI (nM)	%Fast	k_{fast}	k_{slow}	R^2
2.125	ND	0.000457	0.000165	0.9758
4.25	3.796	0.003500	0.000365	0.9848
8.5	6.532	0.010550	0.000847	0.9966
17	9.213	0.057860	0.000986	0.9976
34	11.782	0.090260	0.002100	0.9968
68	28.438	0.257100	0.009340	0.9976
136	49.324	0.764300	0.017050	0.9980
272	69.239	1.098400	0.065980	0.9980
544	86.590	1.328000	0.089420	0.9990

Kinetics of P_{700} re-reduction based on Cyt c_6 concentration

In most cyanobacteria P_{700}^+ is re-reduced via cyt c_6 in vivo. This process is similar to the activity of plastocyanin in plants and algae (Hervas et al. 1995). We have over-expressed and purified the mature, holoform of cyt c_6 that contains a c-terminal His-tag, and used this purified recombinant cyt c_6 to reduce P_{700}^+. The cytochrome is then re-reduced slowly via sodium ascorbate (data not shown). In the absence of cyt c_6, reduction of P_{700}^+ did not occur within our timeframe of our experimental regime (Fig. 5a, bottom trace). The reduction rates of P_{700}^+ were analyzed with both single and double exponential models and the residuals were determined. As can be seen from the amplitude of the residuals, the single exponential fit of the data was unable to accommodate the data adequately especially in the first 100 ms. (Fig. 5a), suggesting an additional component relative to previously reported rates in the reduction rate of P_{700}^+ by cyt c_6 of *T. elongatus*. We find that the amplitude or contribution of this fast phase does not change much as we increase the cyt c_6/PSI ratio and stay around 10 % of the total amplitude. The small contribution of the fast phase is consistent with our two-phase model, such that the slow phase (k_{slow}) closely matches the single exponential rate (k_{obs}), where they both increase linearly with increasing cytochrome concentration and at low cyt c_6 concentration, accounts for the majority of the reduction process, while the rate of the fast phase (k_{fast}) increases with increased cyt c_6 concentration in a single exponential manner (Fig. 5b). We report a value of 3.7×10^7 (M^{-1} s^{-1}) for the observed rate constant with cytochrome concentration ranging from 35 nM to 3.5 µM (Fig. 5b).

Higher temperature increases P_{700} re-reduction kinetics

Measurement temperature was also analyzed, ranging from 5 to 60 °C, showing a similar trend in a linear increase in k_{slow} and a single exponential increase in k_{fast} with increasing temperature (Fig. 6a). The temperature dependence of the k_{slow} is shown at three different protein ratios, all of which display similar rate increases (Fig. 6b). Samples measured at 5 and 60 °C showed similar absorbance amplitudes, indicating that both proteins were still active and stable, while higher temperatures of 65 and 70 °C gave much lower amplitudes that continued to decrease with time (not shown), indicating possible protein degradation

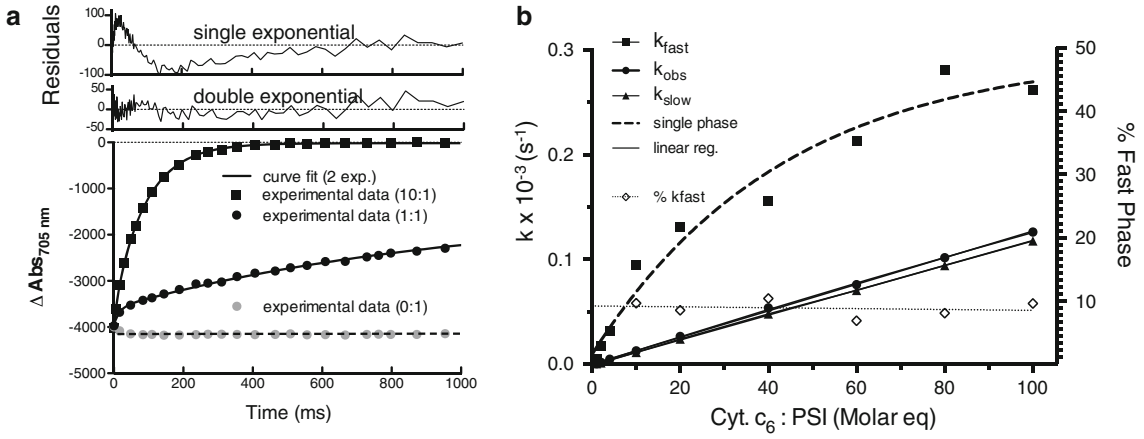

Fig. 5 Total P_{700} re-reduction as a function of cytochrome c_6 concentration (molar excess). **a** 35 nM of PSI was used with 0-,1-, and ten-fold molar excess of cytochrome. Residuals of P_{700} re-reduction shows better fit to two phases as compared to one. **b** 35 nM of PSI was used with excess molar ratios of cytochrome ranging from 0 to 100. Rates of two phases (k_{fast} and k_{slow}) compared to single-phase rate (k_{obs}). K_{fast} fits to a single exponential while k_{slow} and k_{obs} follows a linear fit. The % k_{fast} shows all ratios have about 10 % fast phase

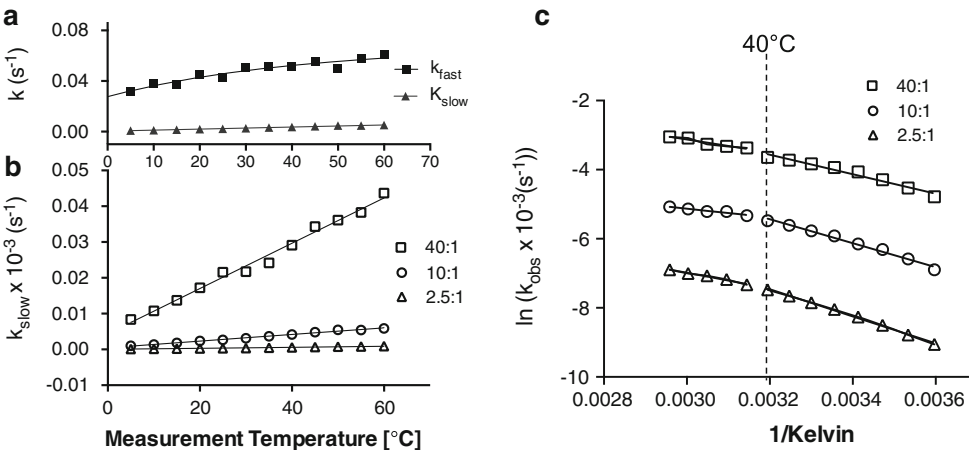

Fig. 6 Temperature dependence of the observed rate constant at three different ratios of cyt c_6 to PSI. **a** As temperature goes from 5 to 60 °C, there is a linear increase in k_{slow} and single exponential increase in k_{fast}, with $\%k_{fast}$ ~10 % (not shown). **b** Increased P_{700} reduction rate (k_{slow}) as the measurement temperature is raised from 5 to 60 °C for 2.5-, 10-, and 40-fold molar excess of cytochrome to PSI. **c** Arrhenius plot shows possible inflection point between 40 and 45 °C

or irreversible unfolding. The temperature effect was also plotted onto an Arrhenius plot from which we then calculated the activation energy to be (28.25, 23.10, and 21.69 kJ/mol) for 2.5, 10, and 40 molar excess of cyt c_6: PSI, respectively (Fig. 6c). An inflection point can be seen between 40 and 45 °C. This is close to the physiological temperature that the PSI source organism was grown at (50 °C) but is much higher than the temperature that we used to culture the *E. coli* for over-expression of the cyt c_6. It is possible that there is some thermally induced conformation change in one or both of these proteins that caused the E_a to become somewhat less above 40 °C. This observation is similar to what has been observed for both plastocyanin and cyt c_6 when tested from the thermophile *Phormidium,* where they also observed that the rate plateaued around 59 °C, with a similar inflection point seen right above 40 °C (Balme et al. 2001).

P700 re-reduction kinetics was affected by pH and ionic strength

The $P700^+$ reduction rate increased with decreasing pH (8.2–5.5) (Fig. 7a), which agrees with previous reports utilizing similar donor proteins with pI's around that of *T. elongatus* cyt c_6 (5.5) (Takabe et al. 1983; Hervas et al. 1992; Medina et al. 1993). In addition to varying pH, changing the buffer composition between MES and TES also appears to have an added effect as seen in Fig. 7a,

where two separate fits are used for the two buffers between pH's of 6.6 and 6.9. Effects of ionic strength also agreed with previous reports (Balme et al. 2001) with a rise in $P700^+$ reduction rate with increasing ionic strength by increasing $MgCl_2$ concentration which reaches a plateau of about 30 mM (Fig. 7b). This has been interpreted as the weakening of any repulsive electrostatic forces between cyt c_6 and PsaF subunit of PSI that might be repulsive (Balme et al. 2001).

LED flash photolysis duration adds secondary phase to P_{700} re-reduction kinetics

Laser flash photolysis was performed on the same sample measured in the JTS-10 with the LED actinic source. Although the probe beam of the YAG laser-based system was 830 nm, we demonstrate that 705 nm and 810 nm detection on the JTS yield virtually identical $P_{700}{}^+$ reduction kinetics (Fig. 8). The measured change in absorbance at 705 nm and 810 nm correlated well with difference spectra of *T. elongatus* P_{700} from previous reports, showing that the absorption change to be about 8 times more intense at 705 nm and in the negative direction (Nakamura et al. 2011). The bleaching at 705 nm is the disappearance of P_{700} while the concomitant appearance of the broad 800–840 nm peak is the direct observation of $P_{700}{}^+$. Results for each cyt c_6: PSI ratio showed similar total $P_{700}{}^+$ recovery times for both actinic light sources, with the main difference being in the curve fit of the laser data showing a single phase in re-reduction as compared with the JTS-10′s two phases (Fig. 4d; Table 2). At each cyt c_6:PSI ratio, the curves shown in Fig. 4d were normalized, with 100 percent being the maximal absorbance change, since the exact same sample was used for both the laser and LED (JTS) systems.

In order to detect a measurable signal with our laser system, the chlorophyll content had to be increased more than ten-fold to 544 nM (48 μg chlorophyll ml^{-1}) and with that caveat, the same sample was then analyzed using the LED-based JTS-10 yielding an unexpected increase in the

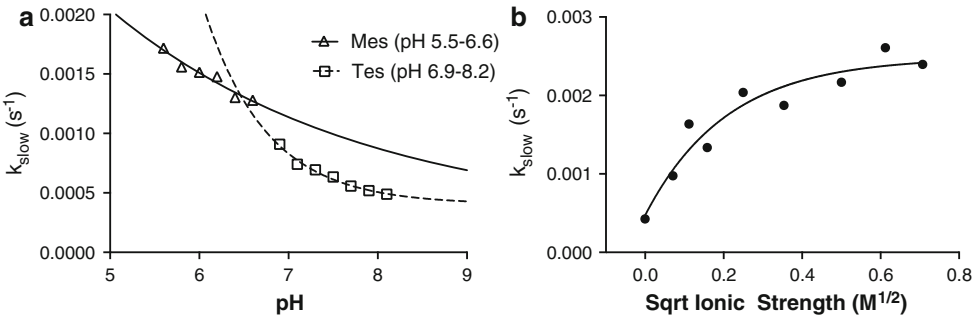

Fig. 7 Effect of pH and ionic strength on reduction rates. **a** Rate decreases as pH increases (5.5–8.2). Data with MES and TES buffer fit to two different exponential fits. **b** Rate increases and plateaus with increasing ionic strength (0–50 mM $MgCl_2$)

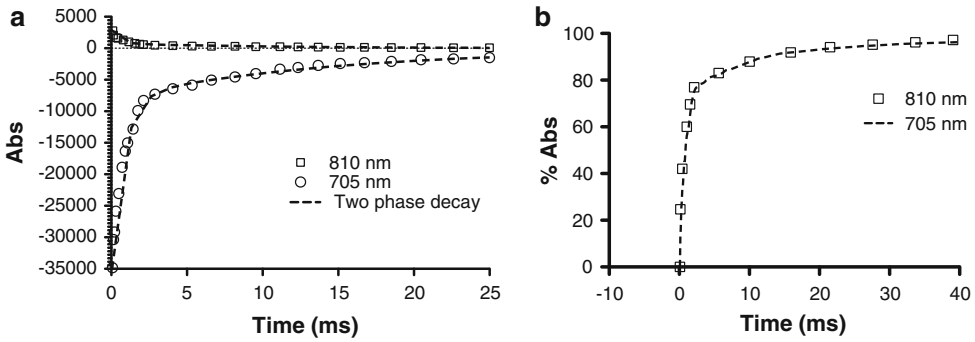

Fig. 8 Comparison of P_{700} reduction rate as a function of measurement wavelength. **a** 705 nm shows about 8 times the change in amplitude of absorbance in the negative direction as 810 nm, with 544 nM PSI and a cyt:PSI of 10:1. **b** Superimposition of normalized re-recovery curves

Table 2 Values from the single and two exponential kinetic fits as shown in Fig. 4d, including the goodness of each fit (R^2)

544 nM PSI	JTS-10 (two exponential fit)				Laser (single exponential fit)	
Cyt:PSI	%Fast	k_{fast}	k_{slow}	R^2	k	R^2
10:1	86.63	1.34	0.09227	0.9989	0.4841	0.9943
20:1	88.34	1.69	0.139	0.994	0.8663	0.9831
40:1	85.04	1.85	0.344	0.9912	1.336	0.9808

percent k_{fast} of our biphasic results (Fig. 4c). This led to the analysis of the contribution of the fast phase of the P_{700}^+ reduction rate as with increased total PSI concentration from 20 to 544 nM, keeping cyt c_6:PSI ratio constant, resulting in the rise of $\%k_{fast}$ from less than 10 % to nearly 90 %. As shown by Fig. 4b, both the fast and slow components of PSI recovery are shown to increase with increasing total protein concentration (PSI and cyt c_6) even with the ratio of cyt c_6:PSI (10:1) being kept constant. We wanted to distinguish the effect of increased total protein concentration, which increases the P700 reduction rates from the true "molecular crowding," with the addition of a foreign crowding agent, which affects the P700 reduction rates by altering the cyt c_6 to PSI interaction. This is further shown in S. Fig. 4, as we plot the fast and slow phase with increasing crowding agent (PEG10 k) compared to that of an increase of the two proteins involved in oxidation and reduction (PSI and cyt c_6) for this assay. The slow phase of the flash photolysis with PEG as a crowding agent shows very little change as we increase the %PEG (open triangles), but there is an exponential increase of the slow phase when the %PSI (open squares) is increased. There is a slight linear increase in the fast phase of the PEG (closed triangle) as compared to exponential increase seen with the increase in %PSI (closed square). With this assay, we wanted to make a clear distinction between adding a foreign crowding agent (PEG10 k) that does not contribute to the oxidation or reduction of PSI versus raising both the %PSI (and cyt c_6) within the sample solution, with the ratio of cyt:PSI kept constant.

Discussion

In our investigation of the electron transfer between recombinantly expressed *T. elongatus* cytochrome c_6 and purified PSI, we utilized a pulsed LED spectrophotometer to monitor the reduction profile of P_{700}^+. As seen from the results we can conclude that with adequate light intensity and duration, the system reaches a maximal ΔAbs_{705nm} or saturation level of P_{700} oxidation. The rate of P_{700}^+ reduction was monitored as a function of electron donor (cyt c_6) concentration, resulting in a recovery curve exhibiting two kinetic components. This suggested either two competing processes or a multiple step process of P_{700}^+ reduction. At ~35 nM PSI, we see that the slower component closely resembles that of the overall or combined rate constant, k observed (k_{obs}), increasing linearly with higher amounts of cyt c_6, suggesting a predominant diffusion-driven system. The faster component was negligible accounting for ~10 % of the total decay amplitude. Reported rate constants for P_{700}^+ reduction by cyt c_6 of *T. elongatus* range from 1.7×10^6 (M^{-1} s^{-1}) (Hatanaka et al. 1993) to 5.9×10^6 (M^{-1} s^{-1}) (Proux-Delrouyre et al. 2003), in which the variability can be attributed to variations in sample set-up and measurement conditions. The linear increase in the k_{slow} and k_{obs} indicates that this system is either at dilute sub-saturating concentrations of cyt c_6 or the interaction is collisional and saturation is not expected.

With previous reports suggesting that cyanobacterial PSI lacks specificity for its electron donor (Hervas et al. 2005), we are surprised to see the biphasic nature of the P_{700}^+ reduction kinetics since the interaction appears to be collisional. This suggested an instrument/light source-specific origin where the longer actinic duration in the millisecond time frame is the main factor.

This is further supported by the same trend in rate increase as we raised the measurement temperature from 5 to 60 °C. The activation energy (E_a) can be further extrapolated by plotting the rate increase on an Arrhenius plot, which yielded a higher E_a for lower cyt c_6 concentrations. This suggested that more energy is required for this reaction when lower electron donor is present.

The dependence of P_{700}^+ reduction kinetics was then investigated as a function of pH; we then created a pH profile showing the highest rate at pH 5.5, which steadily decreases as the pH is raised to 8.2. This effect of pH on the rate of electron transfer correlated with previously described results (Takabe et al. 1983; Hervas et al. 1992; Medina et al. 1993), all of which seem to agree that the lower the pH givesthe donor protein a favorable charge with their pI's all fairly lower than 7. Depending on the source organism, this will vary with regards to any electrostatic surface charges of cyt c_6 and the respective PsaF subunit on the lumen of PSI (Hippler et al. 1999; Sommer et al. 2006). Along with a pH effect, we also see that the rates can be affected by varying the sample buffer composition, between MES and TES. This has been observed in other studies dealing with similar proteins to generate a difference in end-product yield (H_2) (Ellis and Minton 2006; Lubner et al. 2011).

Molecular crowding or total protein density can impact kinetic rates via two contributions. One, large macromolecules will occupy more volume, creating an increased effective concentration, thereby increasing reaction rates. The other opposing effect is that the higher viscosity results in decreased protein diffusion (Ellis and Minton 2006; Kirchhoff 2008). Many kinetic models have been described for the donor/PSI interaction, with variability being attributed to the different source organisms (Hervas et al. 1994, 1995, 2005). In eukaryotes, the electron donor to PSI is predominantly acidic, interacting with a well-conserved positively charged docking site on the N-terminus of PSI's PsaF subunit via electrostatic interactions (Ben-Shem et al. 2003; Hervas et al. 2003). This has been suggested by

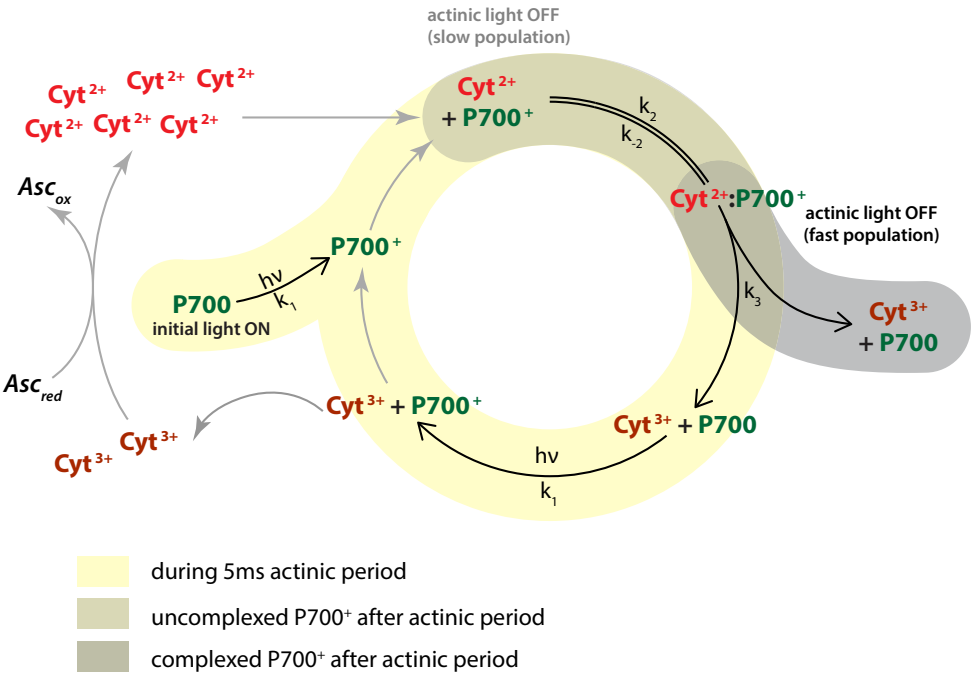

Fig. 9 Schematic of proposed kinetic model for Photosystem I reduction via cytochrome c_6. Measurement of P_{700}^+ reduction after 5 ms actinic period is shown in gray with k_2 and k_3, while multiple P_{700} oxidation/reduction turnovers are depicted in yellow during actinic light on, such that P_{700}^+ pool is fully oxidized. As actinic light (*hv*) oxidizes P_{700} to P_{700}^+, a pre-complex population of $[cyt^{2+} + P_{700}^+]$ is available, leading to $[cyt^{2+}{:}P_{700}^+]$ complex formation represented as k_2 rate constant. The electron transfer event from $[cyt^{2+}{:}P_{700}^+]$ to $[cyt^{3+} + P_{700}]$ is shown as k_3

previous studies to result in a biphasic kinetic rate where the electron transfer of the preformed donor/PSI complex gives rise to the initial fast phase and the following slow phase is attributed to donor/PSI complex formation (Hervas et al. 1995; Fromme et al. 2003; Hervas et al. 2003). This is not the case for cyanobacterial systems however, where a simpler diffusion-based collisional mechanism is thought to exist for electron transfer from donor to PSI, suggesting that the kinetic rates would be better fitted to monophasic model in single-turnover experiments that utilizes an actinic laser (Hervas and Navarro 2011) .

In further analyzing the longer flash duration used in the JTS-10, we see that the light history, along with total protein concentration plays a role in determining the kinetic behavior of the system. As both protein concentrations are increased, keeping the cyt:PSI ratio constant, we see an added effect of increased rates. To compare our results with multiple turnovers, we performed flash photolysis with a laser system with an actinic flash duration of only 6–9 ns, allowing only a single turnover of P_{700}. In this analysis, even with a similar rate of P_{700} recovery, we are able to see only one phase, which would represent a simple collision rate of cyt c_6 to P_{700} as dominated by the second-order rate constant of complex formation. We attribute this kinetic difference to the relatively long actinic light source duration where the system will undergo multiple P_{700} turnovers of oxidation/reduction.

During prolonged illumination, P_{700} is photo-oxidized very rapidly, and the majority of the P_{700} population accumulates in oxidized state regardless of cyt c_6 concentration. In this regime, the oxidized P_{700}^+ may have a different affinity for cyt^{2+} and in any case as its concentration is increased and the equilibrium is shifted toward complex formation. The cycle of $(cyt^{2+} + P_{700}^+ \rightarrow cyt^{3+} + P_{700})$ can have various contributing rates (Fig. 9). If $k_{-2} < k_3 < k_1$, the complex will arrive at a non-zero concentration-dependent steady state and k_3 will become directly observable. As the total protein concentration increases, the complex formation between cyt^{2+} and P_{700}^+ is also favored, further increasing the pool of [cyt: P_{700}], leading to a higher percentage of the fast k_3 phase being observed versus the slower complex formation of k_2. Within one 5 ms P_{700} oxidation/reduction cycle, it is suspected that the conversion of cyt^{2+} to cyt^{3+} is much less than 10 % of the total [cyt c_6], where ascorbate is in excess, leading to cyt^{2+} depletion to be insignificant. The inverse also holds true when we decrease the protein concentration to more dilute conditions and the percent of the fast phase lowered with each dilution where the cyt: P_{700} pool is lessened (Fig. 9; Table 1). While these observations differ from single-turnover laser-based observations, the sensitivity is much greater, requiring much less sample, and more importantly, the direct observation of the first-order decay of the electron transfer is possible. This situation is precluded by the single-turnover experiment, which requires a sequential formation of each population, of which the first is a relatively low probability event, and eliminates the observation of the second faster step.

We find that although the variation exists between our LED-based JTS-10 configuration and a laser-based system, the ability to conduct experiments at lower protein concentrations is a significant advantage of the simpler system

as demonstrated (Fig. 4; Table 1). However, we should add that for experiments with sub-microsecond characteristic times, the ability of the laser-based systems coupled with ultrafast detection will still be most appropriate (Joliot and Joliot 1999; Guergova-Kuras et al. 2001; Xu et al. 2003; Dashdorj et al. 2005). However, the ability to use a common commercially available instrument with fixed optical and detector specifications for these kinetic measurements will enable a more direct comparison between labs worldwide.

Acknowledgments We would like to thank R. Carter, and Dr. Non Chotewutmontri for critically reading the manuscript. BDB and PDF acknowledge support from TN-SCORE, a multidisciplinary research program sponsored by NSF-EPSCoR (EPS-1004083). KN and B.D.B. acknowledge support from the UTK BCMB Department and from the Gibson Family Foundation. KN was supported as an IGERT Fellow from the National Science Foundation IGERT program (DGE-0801470 to BDB and PDF). BDB and KN also acknowledge support from the Directors Strategic Initiative, "Understanding Photo-system I as a Biomolecular Reactor for Energy Conversion" at the Army Research Laboratory, Adelphi, MD (ARL Contract No. W911NF-11-2-0029).

References

Baker DR, Manocchi AK, Lamicq ML, Li M, Nguyen K, Sumner JJ, Bruce BD, Lundgren CA (2014) Comparative photoactivity and stability of isolated cyanobacterial monomeric and trimeric Photosystem I. J Phys Chem B 118(10):2703–2711

Balme A, Hervas M, Campos LA, Sancho J, De la Rosa MA, Navarro JA (2001) A comparative study of the thermal stability of plastocyanin, cytochrome c(6) and photosystem I in thermophilic and mesophilic cyanobacteria. Photosynth Res 70(3):281–289

Beissinger M, Sticht H, Sutter M, Ejchart A, Haehnel W, Rosch P (1998) Solution structure of cytochrome c_6 from the thermophilic cyanobacterium Synechococcus elongatus. EMBO J 17(1):27–36

Ben-Shem A, Frolow F, Nelson N (2003) Crystal structure of plant photosystem I. Nature 426(6967):630–635

Blankenship RE (2002) Molecular mechanisms of photosynthesis. Blackwell, Oxford

Bohner H, Bohme H, Boger P (1980) Reciprocal formation of plastocyanin and cytochrome c-553 and the influence of cupric ions on photosynthetic electron transport. Biochim Biophys Acta 592(1):103–112

Brettel K, Leibl W (2001) Electron transfer in photosystem I. Biochim Biophys Acta 1507(1–3):100–114

Dashdorj N, Xu W, Cohen RO, Golbeck JH, Savikhin S (2005) Asymmetric electron transfer in cyanobacterial Photosystem I: charge separation and secondary electron transfer dynamics of mutations near the primary electron acceptor A0. Biophys J 88(2):1238–1249

De la Rosa MA, Navarro JA, Diaz-Quintana A, De la Cerda B, Molina-Heredia FP, Balme A, Murdoch Pdel S, Diaz-Moreno I, Duran RV, Hervas M (2002) An evolutionary analysis of the reaction mechanisms of photosystem I reduction by cytochrome c(6) and plastocyanin. Bioelectrochemistry 55(1–2):41–45

Diaz-Quintana A, Navarro JA, Hervas M, Molina-Heredia FP, De la Cerda B, De la Rosa MA (2003) A comparative structural and functional analysis of cyanobacterial plastocyanin and cytochrome c (6) as alternative electron donors to Photosystem I. Photosynth Res 75(2):97–110

Ellis RJ, Minton AP (2006) Protein aggregation in crowded environments. Biol Chem 387(5):485–497

Fromme P, Melkozernov A, Jordan P, Krauss N (2003) Structure and function of photosystem I: interaction with its soluble electron carriers and external antenna systems. FEBS Lett 555(1):40–44

Gourovskaya KN, Mamedov MD, Vassiliev IR, Golbeck JH, Semenov AY (1997) Electrogenic reduction of the primary electron donor P700+in photosystem I by redox dyes. FEBS Lett 414(2):193–196

Guergova-Kuras M, Boudreaux B, Joliot A, Joliot P, Redding K (2001) Evidence for two active branches for electron transfer in photosystem I. Proc Natl Acad Sci USA 98(8):4437–4442

Gupta R, He Z, Luan S (2002) Functional relationship of cytochrome c(6) and plastocyanin in Arabidopsis. Nature 417(6888):567–571

Hatanaka H, Sonoike K, Hirano M, Katoh S (1993) Small subunits of Photosystem I reaction center complexes from Synechococcus elongatus. I. Is the psaF gene product required for oxidation of cytochrome c-553? Biochim Biophys Acta 1141(1):45–51

Hervas M, Navarro JA (2011) Effect of crowding on the electron transfer process from plastocyanin and cytochrome c_6 to photosystem I: a comparative study from cyanobacteria to green algae. Photosynth Res 107(3):279–286

Hervas M, De la Rosa MA, Tollin G (1992) A comparative laser-flash absorption spectroscopy study of algal plastocyanin and cytochrome c552 photooxidation by photosystem I particles from spinach. Eur J Biochem 203(1–2):115–120

Hervas M, Ortega JM, Navarro JA, Delarosa MA, Bottin H (1994) Laser flash kinetic-analysis of synechocystis Pcc-6803 cytochrome C(6) and plastocyanin oxidation by Photosystem-I. Biochim Biophys Acta 1184(2–3):235–241

Hervas M, Navarro JA, Diaz A, Bottin H, De la Rosa MA (1995) Laser-flash kinetic analysis of the fast electron transfer from plastocyanin and cytochrome c_6 to photosystem I. Experimental evidence on the evolution of the reaction mechanism. Biochemistry 34(36):11321–11326

Hervas M, Navarro JA, De La Rosa MA (2003) Electron transfer between membrane complexes and soluble proteins in photosynthesis. Acc Chem Res 36(10):798–805

Hervas M, Diaz-Quintana A, Kerfeld CA, Krogmann DW, De la Rosa MA, Navarro JA (2005) Cyanobacterial Photosystem I lacks specificity in its interaction with cytochrome c(6) electron donors. Photosynth Res 83(3):329–333

Hippler M, Drepper F, Haehnel W, Rochaix JD (1998) The N-terminal domain of PsaF: precise recognition site for binding and fast electron transfer from cytochrome c_6 and plastocyanin to photosystem I of *Chlamydomonas reinhardtii*. Proc Natl Acad Sci USA 95(13):7339–7344

Hippler M, Drepper F, Rochaix JD, Muhlenhoff U (1999) Insertion of the N-terminal part of PsaF from *Chlamydomonas reinhardtii* into photosystem I from *Synechococcus elongatus* enables efficient binding of algal plastocyanin and cytochrome c_6. J Biol Chem 274(7):4180–4188

Ho KK, Krogmann DW (1984) Electron donors to P700 in cyanobacteria and algae: an instance of unusual genetic variability. Biochim Biophys Acta 766(2):310–316

Iwuchukwu IJ, Vaughn M, Myers N, O'Neill H, Frymier P, Bruce BD (2010) Self-organized photosynthetic nanoparticle for cell-free hydrogen production. Nat Nanotechnol 5(1):73–79

Jin MX, Yao ZJ, Mi HL (2001) Multi-phasic kinetics of P700(+) dark re-reduction in *Nicotiana tabacum*. Photosynthetica 39(3):419–425

Joliot P, Joliot A (1999) In vivo analysis of the electron transfer within photosystem I: are the two phylloquinones involved? Biochemistry 38(34):11130–11136

Keren N, Aurora R, Pakrasi HB (2004) Critical roles of bacterioferritins in iron storage and proliferation of cyanobacteria. Plant Physiol 135(3):1666–1673

Kirchhoff H (2008) Molecular crowding and order in photosynthetic membranes. Trends Plant Sci 13(5):201–207

Kranz R, Lill R, Goldman B, Bonnard G, Merchant S (1998) Molecular mechanisms of cytochrome c biogenesis: three distinct systems. Mol Microbiol 29(2):383–396

Li M, Semchonok DA, Boekema EJ, Bruce BD (2014) Characterization and evolution of tetrameric photosystem I from the thermophilic cyanobacterium *Chroococcidiopsis* sp TS-821. Plant Cell 26(3):1230–1245

Lubner CE, Applegate AM, Knorzer P, Ganago A, Bryant DA, Happe T, Golbeck JH (2011) Solar hydrogen-producing bionanodevice outperforms natural photosynthesis. Proc Natl Acad Sci USA 108(52):20988–20991

Mamedov MD, Gadzhieva RM, Gourovskaya KN, Drachev LA, Semenov A (1996) Electrogenicity at the donor/acceptor sides of cyanobacterial photosystem I. J Bioenerg Biomembr 28(6):517–522

Medina M, Diaz A, Hervas M, Navarro JA, Gomez-Moreno C, de la Rosa MA, Tollin G (1993) A comparative laser-flash absorption spectroscopy study of *Anabaena* PCC 7119 plastocyanin and cytochrome c_6 photooxidation by photosystem I particles. Eur J Biochem 213(3):1133–1138

Molina-Heredia FP, Wastl J, Navarro JA, Bendall DS, Hervas M, Howe CJ, De La Rosa MA (2003) Photosynthesis: a new function for an old cytochrome? Nature 424(6944):33–34

Nakamura Y, Kaneko T, Sato S, Ikeuchi M, Katoh H, Sasamoto S, Watanabe A, Iriguchi M, Kawashima K, Kimura T, Kishida Y, Kiyokawa C, Kohara M, Matsumoto M, Matsuno A, Nakazaki N, Shimpo S, Sugimoto M, Takeuchi C, Yamada M, Tabata S (2002) Complete genome structure of the thermophilic cyanobacterium *Thermosynechococcus elongatus* BP-1. DNA Res 9(4):123–130

Nakamura A, Suzawa T, Kato Y, Watanabe T (2011) Species dependence of the redox potential of the primary electron donor p700 in photosystem I of oxygenic photosynthetic organisms revealed by spectroelectrochemistry. Plant Cell Physiol 52(5):815–823

Olesen K, Ejdeback M, Crnogorac MM, Kostic NM, Hansson O (1999) Electron transfer to photosystem 1 from spinach plastocyanin mutated in the small acidic patch: ionic strength dependence of kinetics and comparison of mechanistic models. Biochemistry 38(50):16695–16705

Proux-Delrouyre V, Demaille C, Leibl W, Setif P, Bottin H, Bourdillon C (2003) Electrocatalytic investigation of light-induced electron transfer between cytochrome c_6 and photosystem I. J Am Chem Soc 125(45):13686–13692

Santabarbara S, Heathcote P, Evans MC (2005) Modelling of the electron transfer reactions in Photosystem I by electron tunnelling theory: the phylloquinones bound to the PsaA and the PsaB reaction centre subunits of PS I are almost isoenergetic to the iron-sulfur cluster F(X). Biochim Biophys Acta 1708(3):283–310

Schlodder E, Hussels M, Cetin M, Karapetyan NV, Brecht M (2011) Fluorescence of the various red antenna states in photosystem I complexes from cyanobacteria is affected differently by the redox state of P700. Biochim Biophys Acta 1807(11):1423–1431

Shinkarev VP, Zybailov B, Vassiliev IR, Golbeck JH (2002) Modeling of the P700+charge recombination kinetics with phylloquinone and plastoquinone-9 in the A1 site of photosystem I. Biophys J 83(6):2885–2897

Sommer F, Drepper F, Haehnel W, Hippler M (2006) Identification of precise electrostatic recognition sites between cytochrome c_6 and the photosystem I subunit PsaF using mass spectrometry. J Biol Chem 281(46):35097–35103

Takabe T, Ishikawa H, Niwa S, Itoh S (1983) Electron transfer between plastocyanin and P700 in highly-purified photosystem I reaction center complex. Effects of pH, cations, and subunit peptide composition. J Biochem 94(6):1901–1911

Wood PM (1978) Interchangeable copper and iron proteins in algal photosynthesis. Studies on plastocyanin and cytochrome c-552 in *Chlamydomonas*. Eur J Biochem 87(1):9–19

Xu W, Chitnis PR, Valieva A, van der Est A, Brettel K, Guergova-Kuras M, Pushkar YN, Zech SG, Stehlik D, Shen G, Zybailov B, Golbeck JH (2003) Electron transfer in cyanobacterial photosystem I:II. Determination of forward electron transfer rates of site-directed mutants in a putative electron transfer pathway from A0 through A1 to FX. J Biol Chem 278(30):27876–27887